



Implementation of Multi level inverter for SEPIC Converter with Grid Connected PV System

MUDDHANA SIREESHA

M-tech Student Scholar

Department of Electrical & Electronics Engineering,
Velaga Nageswara Rao Engineering College, PONNUR;
GUNTUR (Dt); A.P, India.

Mr. A. ARUN KUMAR M.TECH,

Associate Professor

Department of Electrical & Electronics Engineering,
Velaga Nageswara Rao Engineering College, PONNUR;
GUNTUR (Dt); A.P, India.

Abstract— this paper proposes transformer less grid-connected Single Ended Primary Inductance Converter (SEPIC) for photovoltaic generation systems. The photo voltaic cell can be made up of thin-film solar cell array and the Material used for manufacturing solar cells are polycrystalline si and Mon crystalline si, Using this in solar cell array module enhances the potential to generate the electric power for longer time. The photo voltaic cell can be made up of thin-film solar cell array and the Material used for manufacturing solar cells are polycrystalline si and Mon crystalline si, Using this in solar cell array module enhances the potential to generate the electric power for longer time. The developed model can also be used to extract the physical parameters for a given solar PV cell as a function of temperature and solar radiation. PV strings are connected to a SEPIC converter for three-level inverter to produce output voltage in three levels of Vdc. That was equivalent to the amplitude of the triangular carrier signal were used to generate PWM signals for the switches. The simulation work of these SEPIC converter and multi level inverter with grid connected PV system circuits has been done using MATLAB/SIMULINK software.

Index Terms—DC-DC power conversion, voltage multiplier and solar power generation, renewable energy sources

INTRODUCTION

Because of constantly growing energy demand, grid-connected photovoltaic (PV) systems are becoming more and more popular, and many countries have permitted, encouraged, and even funded distributed-power-generation systems. Currently, solar panels are not very efficient with only about 12–20% efficiency in their ability to convert sunlight to electrical power. The efficiency can drop further due to other factors such as solar panel temperature and load conditions. In order to maximize the power derived from the solar panel, it is important to operate the panel at its optimal power point. To achieve this, a maximum power point tracker will be designed and implemented.

The MATLAB/PSPICE model of the PV module is developed [1–4] to study the effect of temperature and insolation on the performance of the PV module. The power electronics interface, connected between a solar

panel and a load or battery bus, is a pulse width modulated (PWM) DC-DC converter or their derived circuits used to extract maximum power from solar PV panel. *I-V* characteristic curve of photovoltaic generators based on various DC-DC converters [5–8] was proposed and concluded that SEPIC converter is the best alternative to track maximum power from PV panel.

The various types of non-isolated DC-DC converters for the photo voltaic system is reviewed [9].

The maximum power tracking for PV panel using DCDC converter is developed [10] without using microcontroller. This approach ensures maximum power transfer under all atmospheric conditions. The analogue chaotic PWM is used to reduce the EMI in boost converter. The conversion efficiency is increased when CPWM is used as a control technique [11]. To increase conversion efficiency, an active clamp circuit is introduced into the proposed one to provide soft switching features to reduce switching losses. Moreover, switches in the converter and active clamp circuit are integrated with a synchronous switching technique to reduce circuit complexity and component counts, resulting in a lower cost and smaller volume [12].

The wide use of fossil fuel has resulted in the emission of green house gases which results in pollution. In spite of the increase in fuel cost there is an increase in renewable energy trading. The run provides the energy needed to sustain life in our system. It is clean, inexhaustible, abundantly, and universally scare of RE. The most popular renewable energy is solar energy, that can be utilized directly in two ways (1) by collecting the radiant heat and using it in a thermal system or (2) collecting and converting it directly to electrical energy using photovoltaic system. The thin-film solar cell has the potential to generate the electric power for longer time, than a crystalline si solar cell and thin film can be easily combined with glass, plastics, metal, and it can be incorporated [13].

The SEPIC converter should operate with high switching frequency. However, as the switching frequency increases, the reverse recovery current of the output diode affects the

switching devices in the form of additional switching losses. Other adverse effects of the reverse-recovery problem include electromagnetic interference (EMI) noises and additional thermal management. Also, the switch utilization factor in the SEPIC converter is much lower than that of other topologies, such as the buck and boost converters. In other words, the power-handling capabilities of the semiconductor devices in the SEPIC converter are much lower than those of the buck or the boost converter at the same power level. Thus, the reduction of reverse recovery loss is particularly important for the SEPIC converter [14].

Different topologies MLIs for the conversion from DC to AC are available such as Neutral point clamped MLI (NPC-MLI), Flying capacitor MLI (FC-MLI), Cascade H-Bridge MLI (CHB-MLI) and Asymmetrical Cascade H-Bridge Multilevel inverters. Among them CHB-MLIs are mostly used for PV applications because each cell of CHBMLI requires separate DC sources which can be easily supplied by individual PV arrays and each H-Bridge cell will be available in a single module. The number of levels of the output wave form increased by cascading the no. of H Bridge cells. There is a large no. of control techniques developed so far to control the operation of multilevel inverters such as SVPWM, SPWM, OHPWM, SHE-PWM, Hybrid modulation [15].

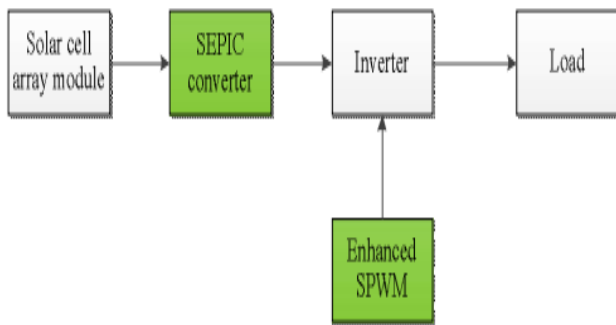


Figure.1. Grid connected converter systems with SEPIC converter. Figure .1.shows that the solar array module producing lower level DC voltage, and this voltage is feedback to input of SEPIC converter Based on the requirement these SEPIC converter performs both boost and buck operation. And this change in voltage is the output of SEPIC converter. This output is passed as a Input to the inverter, to convert the DC voltage to AC voltage and connected to load. The conventional method boost converter is acts as the step-up converter, and the output voltage is greater than the input voltage, and drawback of this method is only the voltage is stepped up and one inductor is used so energy storage is less compare to proposed system SEPIC converter is used in the proposed method. It is a DC-DC converter to allow the electrical potential (voltage) at its

output to be greater than or lesser than the input voltage. It can use coupled inductors and take the form of a single package at cost slightly higher than single inductor. The purpose of inductor is to store the energy in the form of electromagnetic field [5]-[6] Proposed converter is controlled by the duty cycle control method. By increasing duty cycle output voltage can be controlled. The advantage of SEPIC is non-inverted output voltage (the output voltage is of the same polarity as the input voltage).

II.PROPOSED CONVERTER WITHOUT MAGNETIC COUPLING

A. Power Circuit without Magnetic Coupling

The step-up and step-down static gain of the SEPIC converter is an interesting operation characteristic for a wide input voltage range application. However, the switch voltage is equal the sum of the input and output voltages, and the static gain is lower than the classical boost converter. The modification of the SEPIC converter is accomplished adding only two components with the inclusion of the diode D_M and the capacitor C_M , as presented in Fig.2. Many operational characteristics of the classical SEPIC converter are changed with the proposed modification, as the elevation of the converter static gain. The capacitor C_M is charged with the output voltage of the classical boost converter. The polarity of the CS capacitor voltage is inverted in the proposed converter and the expressions

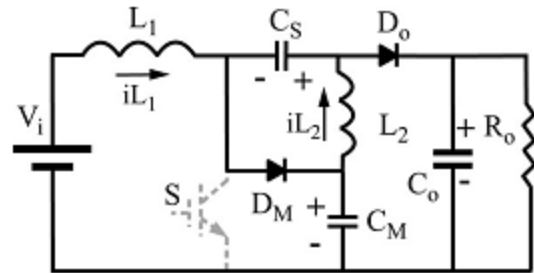


Fig.2. First operation stage.

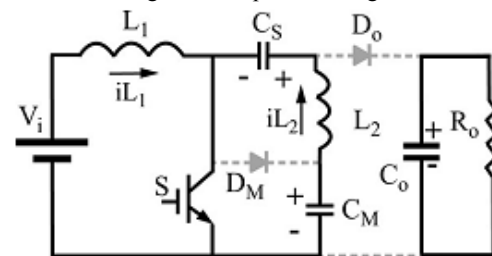


Fig.3. Second operation stage.

of the capacitors voltages and other operation characteristics are presented in the theoretical analysis. The continuous conduction mode (CCM) of the modified SEPIC converter presents two operation stages. All

capacitors are considered as a voltage source and the semiconductors are considered ideals for the theoretical analysis.

1) First Stage [t₀–t₁](Fig.2):At the instantt₀, switch S is turned-off and the energy stored in the input inductor L1 is transferred to the output through the CS capacitor and output diode D_o and also is transferred to the CM capacitor through the diode D_M. Therefore, the switch voltage is equal to the CM capacitor voltage. The energy stored in the inductor L2 is transferred to the output through the diode D_o.

2) Second Stage [t₁–t₂](Fig.3):At the instantt₁, switch S is turned-on and the diodes D_M and D_o are blocked and the inductors L1 and L2 store energy. The input voltage is applied to the input inductor L1 and the voltage V_{CS}–V_{CM} is applied to the inductor L2. The V_{CM} voltage is higher than the V_C voltage. The main theoretical waveforms operating with hard switching commutation are presented in Fig.4. The maximum voltage in all diodes and in the power switch is equal to the CM capacitor voltage. The output voltage is equal to the sum of the CS and CM capacitors voltage. The average L1 inductor current is equal to the input current, and the average L2 inductor current is equal to the output current. The static gain of the proposed converter can be obtained considering null the average inductors voltage at the steady state and it is presented in (1) considering the CCM operation. The static gain of the proposed converter is higher than the obtained with the classical boost

$$\frac{V_o}{V_i} = \frac{1 + D}{1 - D} \quad (1)$$

The CM capacitor voltage is calculated by (2) that is the same output voltage of the classical boost converter. The maximum switch voltage is equal to the V_{CM} voltage. Therefore, the switch

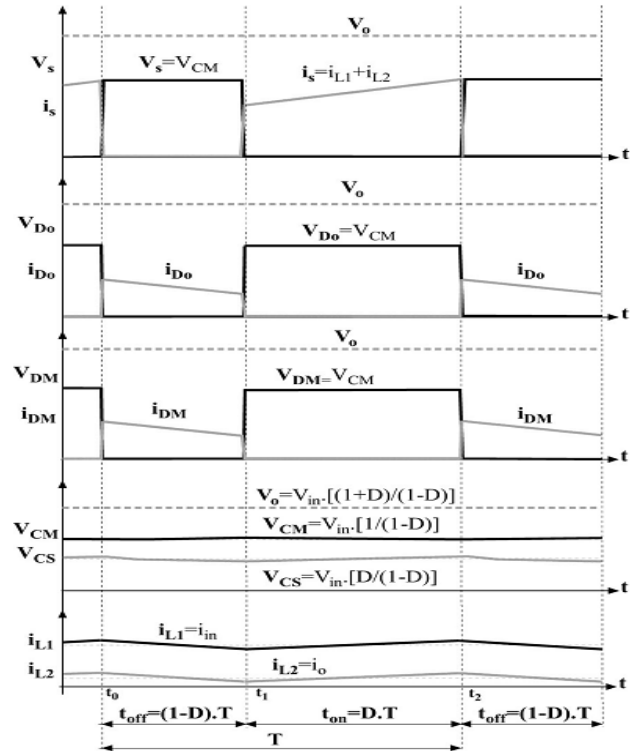


Fig.4. Main theoretical waveform.

Voltage will be lower than the converter output voltage

$$\frac{V_{CM}}{V_i} = \frac{1}{1 - D} \quad (2)$$

The voltage across the CS capacitor is calculated by (3)

$$\frac{V_{CS}}{V_i} = \frac{D}{1 - D} \quad (3)$$

The static gain of the classical SEPIC, boost and modified SEPIC converters are presented in Fig.5 As it can be observed in this figure, with a duty cycle equal to D=0.818, a static gain equal to 10 is obtained, and the switch voltage is equal to 5.5 times the input voltage. Therefore, the switch voltage is close to half of the output voltage. The theoretical analysis, operation stages, and waveforms of the modified SEPIC converter operating in discontinuous conduction mode (DCM) is not presented in this paper. However, the static gain and the CM and CS capacitor voltages operating in DCM are presented in (4), (5), and (6), respectively

$$\frac{V_o}{V_i} = 1 + \frac{V_i \cdot D^2}{2 \cdot i_o \cdot L_{eq} \cdot f} \quad (4)$$

$$\frac{V_{CM}}{V_i} = 1 + \frac{V_i \cdot D^2}{4 \cdot i_o \cdot L_{eq} \cdot f} \quad (5)$$

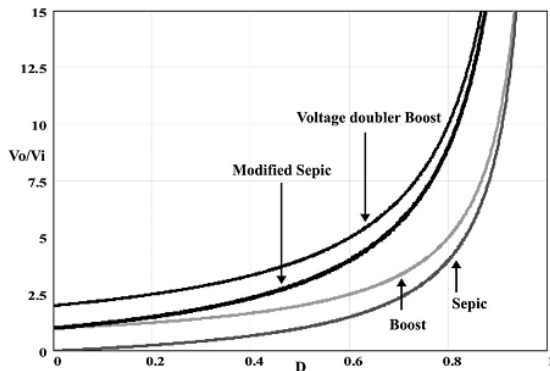


Fig. 5. Converters static gain.

$$\frac{V_{CS}}{V_i} = \frac{V_i \cdot D^2}{4 \cdot i_o \cdot L_{eq} \cdot f} \quad (6)$$

$$L_{eq} = \frac{L_1 \cdot L_2}{L_1 + L_2} \quad (7)$$

III. PROPOSED CONVERTER WITH MAGNETIC COUPLING

A. Power Circuit with Magnetic Coupling

The modified SEPIC converter without magnetic coupling can operate with the double of the static gain of the classical boost converter for a high duty-cycle operation. However, a very high static gain is necessary in some applications. A practical limitation for the modified SEPIC converter in order to maintain the converter performance is a duty cycle close to $D=0.85$, resulting in a maximum static gain equal to $toq=12.3$. A simple solution to elevate the static gain without increasing the duty cycle and the switch voltage is to include a secondary winding in the L_2 inductor. The L_2 inductor operation is similar to a back-boost inductor and a secondary winding can increase the output voltage by the inductor windings turns ratio (n), operating as a fly back transformer. Fig.6 shows this alternative circuit. However, this converter structure presents the problem of over voltage at the output diode D_o due to the existence of the coupling winding L_2 leakage

inductance. The energy stored in the leakage inductance, due to the reverse recovery current of the output diode, results in voltage ring and high reverse voltage at the diode D_o . This overvoltage is not easily controlled with classical snubber or dissipative clamping. A simple solution for this problem is the inclusion of a voltage multiplier at the secondary side as presented in Fig.7. This voltage multiplier increases the converter static gain, the voltage across

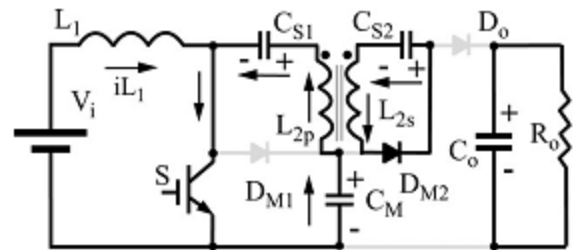


Fig.6. First operation stage.

Diode is reduced to a value lower than the output voltage and the energy stored in the leakage inductance is transferred to the output. Therefore, the secondary voltage multiplier composed by the diode DM_2 and capacitor CS_2 is also a non dissipative clamping circuit for the output diode. The circuit presented in Fig.6 is the power circuit studied in this paper. The solutions based on the classical boost converter with magnetic coupling or the integration of the magnetic coupling and the voltage multiplier cell can present very high voltage gain and an excellent performance as presented in [11]–[12]. However, as the magnetic coupling is accomplished with the input inductor in the boost-based solutions, the input current ripple is significantly increased and depends on the inductor winding turns ratio. Increasing the inductor turns ratio and the static gain, the input current ripple rises. The input current ripple increment is a non desirable operation characteristic for some applications as the fuel cell power source. As the magnetic coupling is not accomplished with the input inductor in the proposed topology, the input current ripple is low and is not changed by the magnetic coupling. There are also some proposed solutions based on the integration of the SEPIC converter with boost and fly back dc–dc converters. An isolated active clamp SEPIC-fly back converter is presented in [13] in order to obtain high efficiency. However, the proposed topology presents pulsating input current, and the active clamp technique increases the converter complexity with an additional controlled switch and command circuit. The integration of the boost converter with a SEPIC converter is also proposed in [14] and [15]. Some operation characteristics of this converter are similar to the circuit with magnetic

coupling proposed in this paper. The main differences of the proposed converter with respect the previous topology are the ZCS switch turn-on obtained with a resonant operation stage, reducing the commutation losses even in the operation with light load and a higher static gain considering the same transformer turns ratio, reducing the converter duty cycle and the switch voltage. The CCM operation of the modified SEPIC converter with magnetic coupling and output diode clamping presents five operation stages. All capacitors are considered as a voltage source, and the semiconductors are considered ideals for the theoretical analysis.

1) First Stage [t0-t1] (Fig.6): The power switch S is conducting and the input inductor L_1 stores energy. The capacitor C_{S2} is charged by the secondary winding L_{2s} and diode DM_2 . The leakage inductance limits the current and the energy transference occurs in a resonant way. The output diode is blocked, and the maximum diode voltage is equal to $(V_o - V_{CM})$. At the

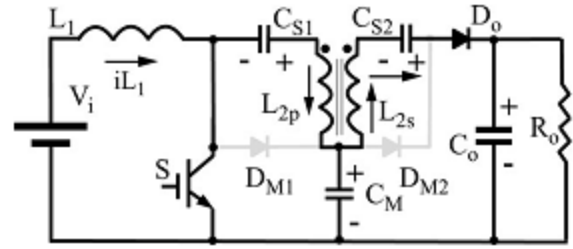


Fig.10. Fifth operation stage.

Instant t_1 , the energy transference to the capacitor C_{S2} is finished and the diode DM_2 is blocked.

2) Second Stage [t1-t2] (Fig 7): From the instant t_1 , when the diode DM_2 is blocked, to the instant t_2 when the power switch is turned OFF, the inductors L_1 and L_2 store energy and the currents linearly increase.

3) Third Stage [t2-t3] (Fig .8): At the instant t_2 the power switch S is turned OFF. The energy stored in the L_1 inductor is transferred to the C_M capacitor. Also, there is the energy transference to the output through the capacitors C_{S1} , C_{S2} inductor L_2 and output diode D_o .

4) Fourth Stage [t3-t4] (Fig.9): At the instant t_3 , the energy transference to the capacitor C_M is finished and the diode DM_1 is blocked. The energy transference to the output is maintained until the instant t_4 , when the power switch is turned ON.

5) Fifth Stage [t4-t5] (Fig.10): When the power switch is turned ON at the instant t_4 , the current at the output diode D_o linearly decreases and the di/dt is limited by the transformer leakage inductance, reducing the diode reverse recovery current problems. When the output diode is blocked, the converter returns to the first operation stage. The main theoretical waveforms of the modified SEPIC converter with magnetic coupling and with the voltage multiplier at the secondary side are presented in Fig.13. The switch voltage and the voltage across all diodes is lower than the output voltage. The power switch turn-on occurs with almost zero current reducing significantly the switching losses. The current variation ratio (di/dt) presented by all diodes is limited due to the presence of the coupling inductor leakage inductance, reducing the negative effects of the diode reverse recovery current.

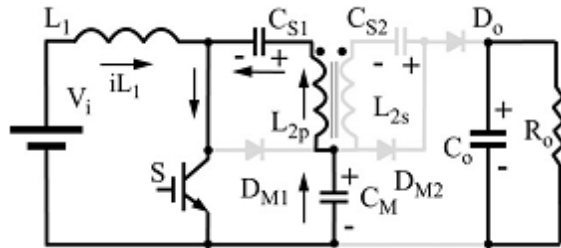


Fig.7. Second operation stage

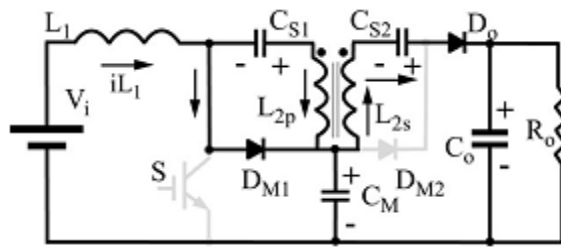


Fig.8. Third operation stage

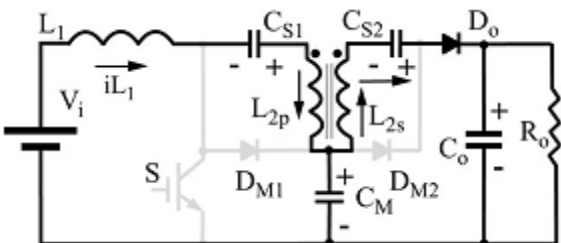


Fig.9. Fourth operation stage.

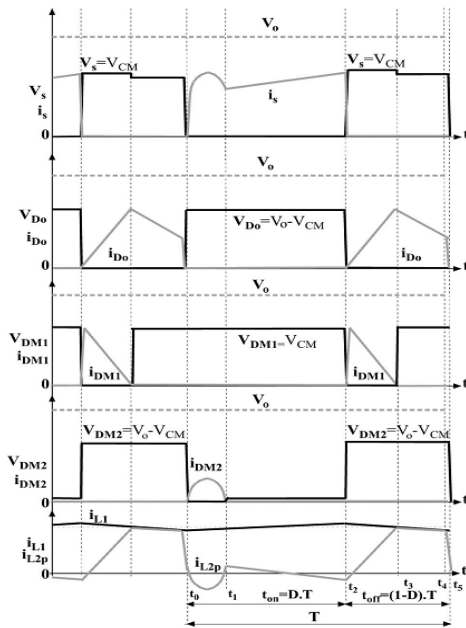


Fig.11. Main theoretical waveforms of the modified SEPIC converter with Magnetic coupling and voltage multiplier at the secondary side.

The static gain of the modified SEPIC converter with magnetic coupling and voltage multiplier is calculated by (8). The static gain can be increased by the windings turns ratio (n) without increasing the switch voltage

$$\frac{V_o}{V_i} = \frac{1}{1-D} \cdot (1+n) \tag{8}$$

Where the inductor windings turns ratio (n) is calculated by

$$n = \frac{N_{L2s}}{N_{L2p}} \tag{9}$$

IV. PHOTOVOLTAIC (PV) SYSTEM

In the crystalline silicon PV module, the complex physics of the PV cell can be represented by the equivalent electrical circuit shown in Fig. 12. For that equivalent circuit, a set of equations have been derived, based on standard theory, which allows the operation of a single solar cell to be simulated using data from manufacturers or field experiments.

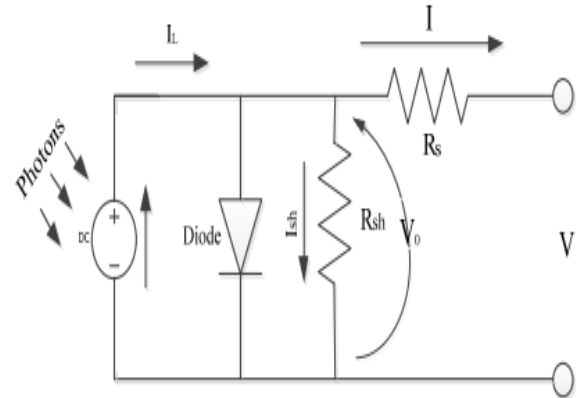


Fig.12. Equivalent electrical circuit of a PV module.

The series resistance RS represents the internal losses due to the current flow. Shunt resistance Rsh, in parallel with diode, this corresponds to the leakage current to the ground. The single exponential equation which models a PV cell is extracted from the physics of the PN junction and is widely agreed as echoing the behaviour of the PV cell

$$I = I_L - I_{st} \left(\exp \left(\frac{V + R_s I}{V_t} \right) - 1 \right) - \frac{V + R_s I}{R_{sh}} \tag{10}$$

The number of PV modules connected in parallel and series in PV array are used in expression. The Vt is also defined in terms of the ideality factor of PN junction (n), Boltzmann's constant (KB), temperature of photovoltaic array (T), and the electron charge (q). Applied dynamical electrical array reconfiguration (EAR) strategy on the photovoltaic (PV) generator of a grid-connected PV system based on a plant-oriented configuration, in order to improve its energy production when the operating conditions of the solar panels are different. The EAR strategy is carried out by inserting a controllable switching matrix between the PV generator and the central inverter, which allows the electrical reconnection of the available PV modules.

V. Diode Clamped Multilevel Inverters

The diode clamped multilevel inverter uses capacitors in series to divide up the dc bus voltage into a set of voltage levels. To produce m levels of the phase voltage, an m level diode clamp inverter needs (m-1) capacitors on the dc bus.

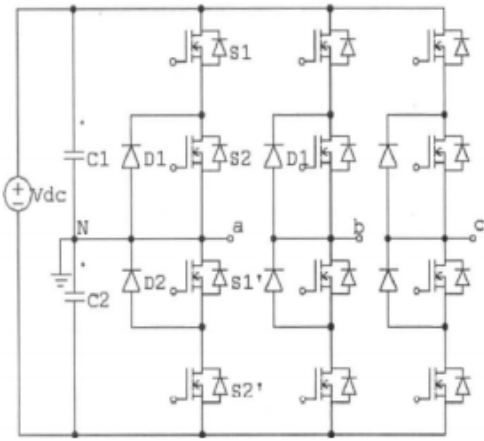


Fig.13. Diode Clamped Three Level Inverter.

In this paper, diode clamped multilevel inverters topology is used shown in fig .13.

VLMATLAB/SIMULINK RESULTS

Here the different cases are presents Case.1.Proposed Converter without Magnetic Coupling. Case.2. Proposed Converter with Magnetic Coupling. Case.3. Proposed Converter with Magnetic Coupling and closed loop controller. Case.4.Proposed Converter with Magnetic Coupling and inverter with grid connected PV.

Case1.Proposed Converter without Magnetic Coupling.

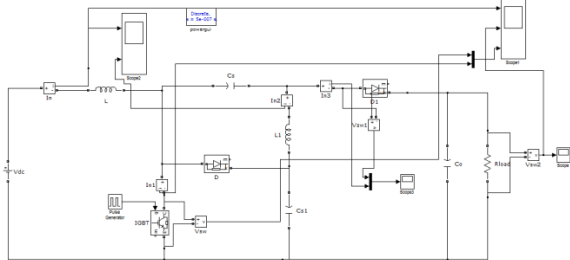


Fig.14.Matlab/Simulink Model of the Modified SEPIC Converter without Magnetic Coupling.

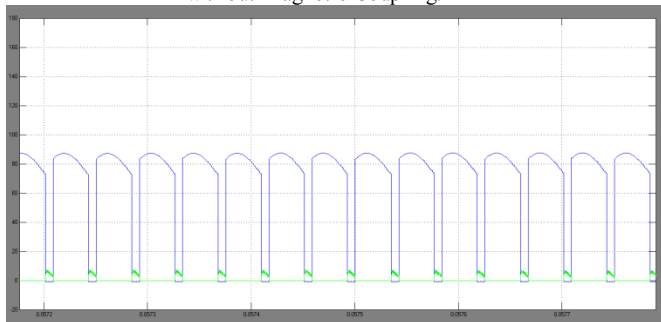


Fig.15. Output diode D0 voltage and current of the modified SEPIC converter without magnetic coupling.

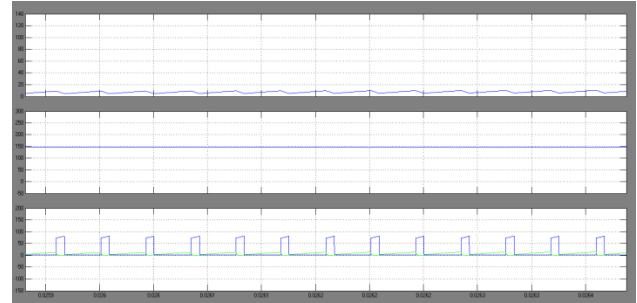


Fig.16. Input current, output voltage, switch current, and voltage of the modified SEPIC converter without magnetic coupling.

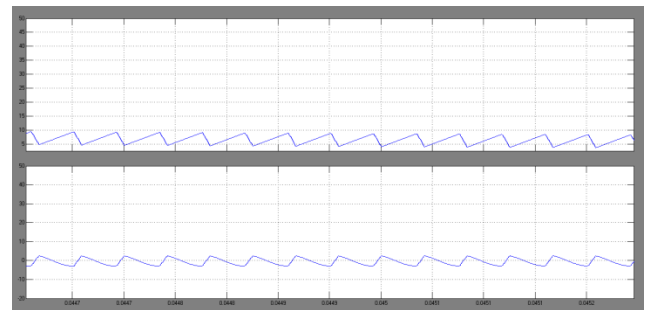


Fig.17. L1 and L2 inductor current of the modified SEPIC converter without magnetic coupling.

Case2. Proposed Converter with Magnetic Coupling.

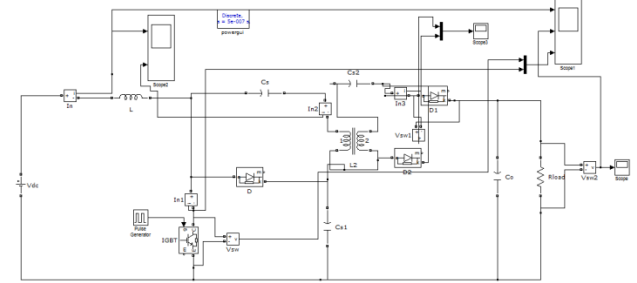


Fig.8.Matlab/Simulink Model of the Modified SEPIC Converter with Magnetic Coupling.

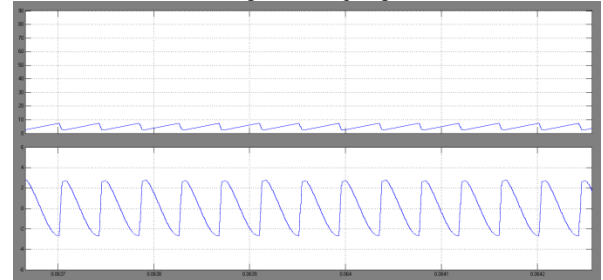


Fig.19. Switch current and switch voltage of the Modified SEPIC converter with magnetic coupling and voltage multiplier.

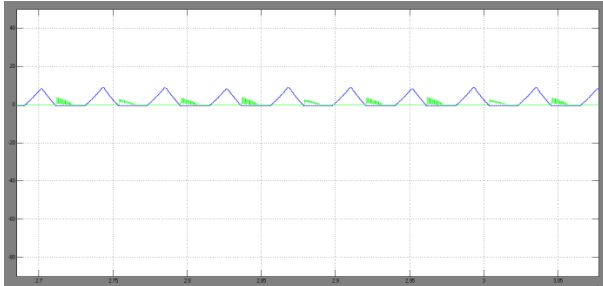


Fig.20. Output diode D_o voltage and current of the modified SEPIC converter with magnetic coupling.

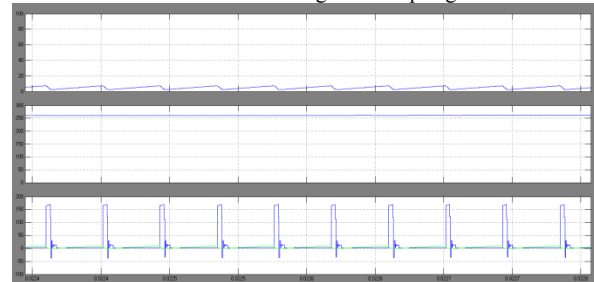


Fig.21. Input current, output voltage, switch current, and switch voltage of the modified SEPIC converter with magnetic coupling and voltage multiplier.

Case3. Proposed Converter with Magnetic Coupling and closed loop controller.

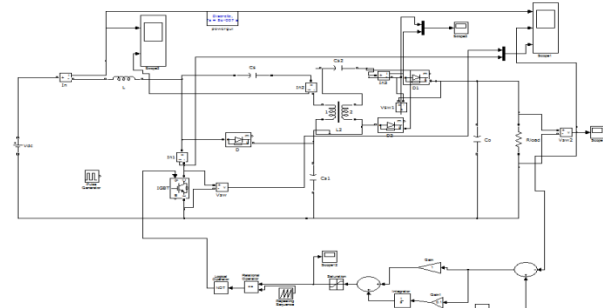


Fig.22. Matlab/Simulink Model of the Modified SEPIC Converter with Magnetic Coupling and closed loop.

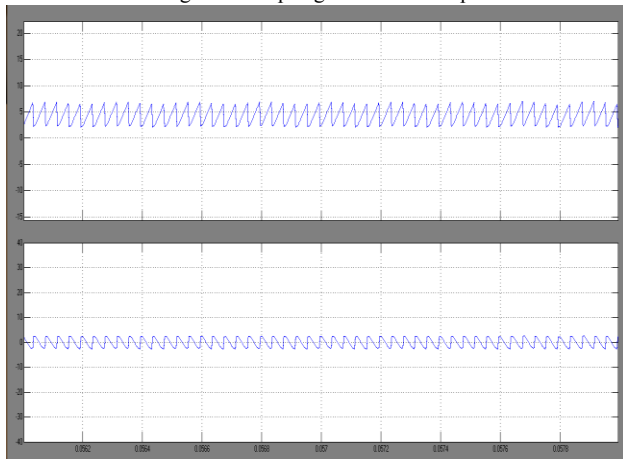


Fig.23. Switch current and switch voltage of the Modified SEPIC converter with magnetic coupling and voltage multiplier.

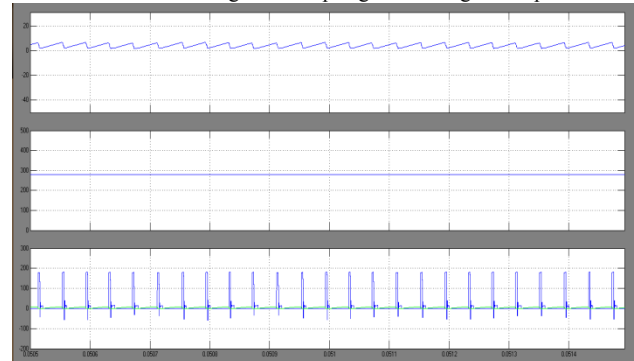


Fig.24. Input current, output voltage, switch current, and switch voltage of the modified SEPIC converter with magnetic coupling and voltage multiplier.

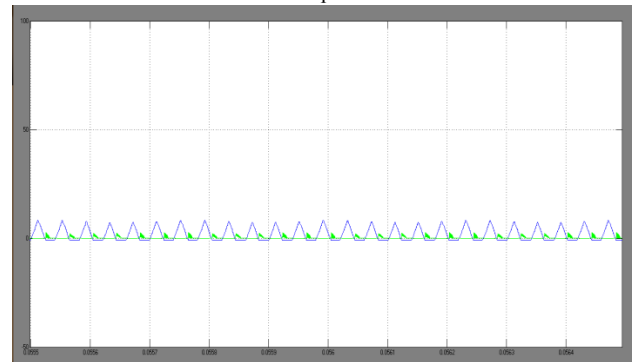


Fig.25. Output diode D_o voltage and current of the modified SEPIC converter with magnetic coupling.

Case4. Proposed Converter with Magnetic Coupling and inverter with grid connected PV.

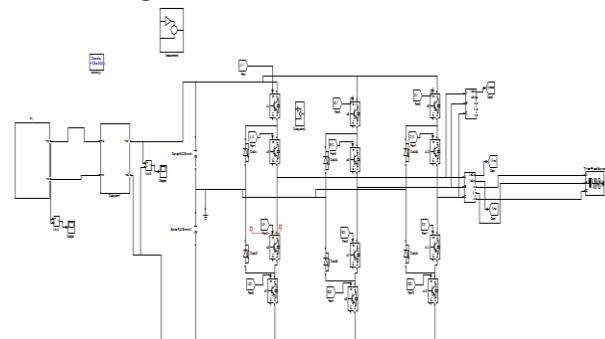


Fig.26. Matlab/Simulink Model of the Modified SEPIC Converter with Magnetic Coupling inverter with grid connected PV.

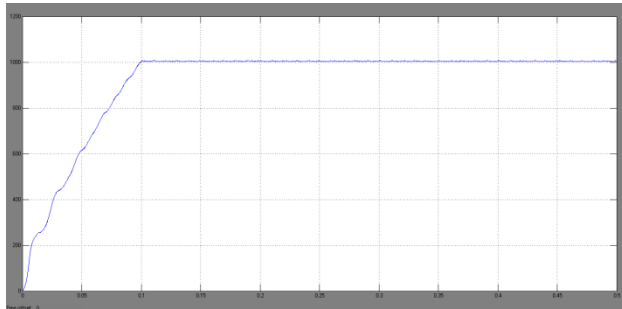


Fig.27.output voltage.

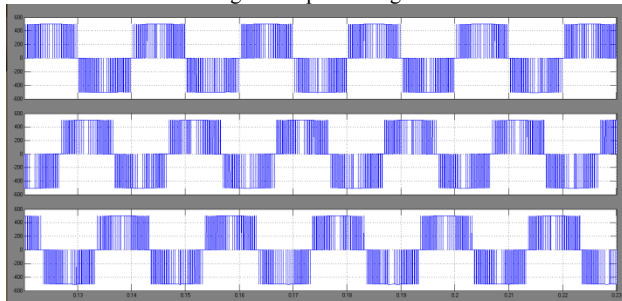


Fig.28 inverter phase to phase voltage.

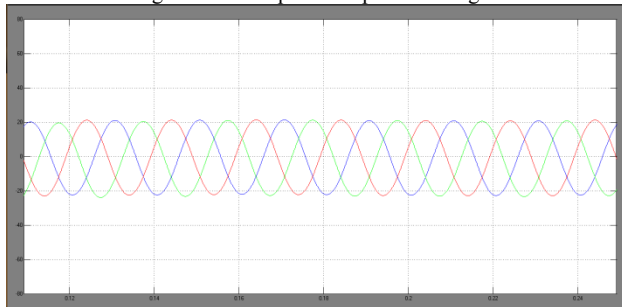


Fig.29. Grid current.

VII. CONCLUSION

Two new topologies of non isolated high static gain converters are presented in this paper. The first topology without magnetic coupling can operate with a static gain higher than 10 with a reduced switch voltage. The structure with magnetic coupling can operate with static gain higher than 20 maintaining low the switch voltage. The circuit topology, control algorithm, and operating principle of the proposed inverter have been analyzed in detail. The configuration is suitable for PV application as the PV strings operate independently and later expansion is possible. This paper presents simulation of multilevel inverter for SEPIC converter with grid connected PV system performs the three level inverter and grid current.

REFERENCES

- [1] E. E. Jimenez-Toribio, A. A. Labour-Castro and F.M.Rodríguez, "Sensorless Control of SEPIC and Cuk Converters for DC Motors using Solar Panels" in proceeding on Electrical Machines and Drives conference, IEMDC-09, 2009, pp 1503-1510.
- [2] J.G. Llorente, E.I. Ortiz-Rivera, A.S. Llinas, "Analysing the Optimal Matching of DC Motors to Photovoltaic Modules via DC-DC Converters"

in proceedings on Applied Power Electronics conference (APEC) ,pp-1062-1068.

[3] M. Veerachary and K. S. Shinoy, "V2- Based Power Tracking for Nonlinear PV Sources" , IEE proceeding on Electrical Power Applications, Vol. 152, No. 5, pp 1263-1270, September 2005.

[4] M. G. Villalva, J.R. Gazoli, E. R. Filho, "Comprehensive Approach to Modeling and Simulation of PV Arrays", IEEE Transactions on Power Electronics, Vo. 24, No. 5, pp 1198-1208, May 2009.

[5] Renewable energy source water pumping systems - A literature review C. Gopal, M.Mohanraj, P. Chandramohan P. Chandrasekar, Elsevier 30 may 2013.

[6] L. Jian, K. T. Chau, and K. T. Chau, "A magnetic geared outer-rotor permanent-magnet brushless machine for wind power generation" IEEE Trans. Ind. Appl., vol. 45, no. 3, pp. 954-962, May/June 2009.

[7] S. Rahmam, M. A. Khallat, and B. H. Chowdhury, "A discussion on the diversity in the applications of photovoltaic system," IEEE Trans. Energy Conversion, vol. 3, pp. 738-746, Dec. 1988.

[8] Y.M. Chen, Y.C. Liu, S.C. Hung, and C.S. Cheng, "Multi-Input Inverter for Grid-Connected Hybrid PV/Wind Power System," IEEE Transactions on Power Electronics, vol. 22, May 2007.

[9] Y. Li, X. Ruan, D. Yang, F. Liu and C. K. Tse, "Synthesis of Multiple-Input DC/DC Converters," IEEE Trans. Power Electron., vol. 25, no. 9, pp. 2372-2385, Sep. 2010.

[10] H. Tao, A. Kotsopoulos, J. L. Duarte, and M. A. M. Hendrix, "Family of multiport bidirectional DCDC converters," Electric Power Applications, IEE Proceedings, vol. 153, pp. 451-458, 2006.

[11] R. J. Wai and R. Y. Duan, "High-efficiency power conversion for lowpower fuel cell generation system," IEEE Trans. Power Electron., vol. 20, no. 5, pp. 847-856, Sep. 2005.

[12] W. Li and X. He, "An interleaved winding-coupled boost converter with passive lossless clamp circuits," IEEE Trans. Power Electron., vol. 22, no. 4, pp. 1499-1507, Jul. 2007.

[13] S. Kim, D.-K. Choi, S.-J. Jang, T.-W. Lee, and C.-Y. Won, "The active clamp SEPIC- flyback converter," in Proc. IEEE 36th Power Electron. Spec. Conf., 2005 (PESC '05), Jun. 2005, pp. 1209-1212.

[14] K. Park, G. Moon, and M.-J. Youn, "Nonisolated high step-up boost converter integrated with SEPIC converter," IEEE Trans. Power Electron., vol. 25, no. 9, pp. 2266-2275, Sep. 2010.

[15] K. Park, H.-W. Seong, H.-S. Kim, G.-W. Moon, and M.-J. Youn, "Integrated boost-SEPIC converter for high step-up applications," in Proc. IEEE Power Electron. Spec. Conf. 2008 (PESC 2008), Jun. 2008, pp. 944-950.